Journal of Molecular Graphics and Modelling 131 (2024) 108806

Contents lists available at ScienceDirect

Journal of Molecular Graphics and Modelling

journal homepage: www.elsevier.com/locate/jmgm

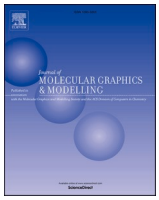

The binding of diruthenium (II,III) and dirhodium (II,II) paddlewheel complexes at DNA/RNA nucleobases: Computational evidences of an appreciable selectivity toward the AU base pairs

Iogann Tolbatov [a,*], Paolo Umari [a], Alessandro Marrone [b]

[a] Department of Physics and Astronomy, University of Padova, via F. Marzolo 8, 35131, Padova, Italy
[b] Dipartimento di Farmacia, Università degli Studi "G. D'Annunzio" Chieti-Pescara, Via dei Vestini, 66100, Chieti, Italy

ARTICLE INFO

Keywords:
DFT
Diruthenium paddlewheel complexes
Dirhodium paddlewheel complexes
DNA/RNA
Metalation

ABSTRACT

Multiple medicinal strategies involve modifications of the structure of DNA or RNA, which disrupt their correct functioning. Metal complexes with medicinal effects, also known as metallodrugs, are among the agents intended specifically for the attack onto nucleosides. The diruthenium (II,III) and dirhodium (II,II) paddlewheel complexes constitute promising dual acting drugs due to their ability to release the therapeutically active bridging ligands upon their substitution by endogenous ligands. In this paper, we study the structure and the stability of the complexes formed by the diruthenium (II,III) and dirhodium (II,II) paddlewheel complexes coordinated in axial positions with the DNA/RNA nucleobases or base pairs, assuming the attainable metalation at all the accessible pyridyl nitrogens. Dirhodium complexes coordinate at the pyridyl nitrogens more strongly than the diruthenium complexes. On the other hand, we found that the diruthenium scaffold binds more selectively to nucleobase targets. Furthermore, we reveal a tighter coordination of diruthenium complex at the adenine-uracil base pair, compared to adenine-thymine, hence constituting a scarce instance of RNA-selectivity. We envision that the here reported computational outcomes may pace future experiments addressing the binding of diruthenium and dirhodium paddlewheel complexes at either single nucleobases or DNA/RNA fragments.

1. Introduction

The deoxyribonucleic acid (DNA) and ribonucleic acid (RNA) biopolymers conceal the genetic instructions for the major processes in living organisms and viruses. The DNA polynucleotides encode the information on how to function, grow, develop, and reproduce these data being stored in the nucleus of eukaryotes [1]. On the other hand, the RNA molecules are employed as a means to transport the commands outside of the nucleus and a blueprint for the formation of proteins (messenger RNA) [2], or some RNA may perform the biological functions themselves (non-coding RNA) [3]. Both DNA and RNA biopolymers constitute the chains of nucleosides held together by a phosphodiester scaffolding; this assembly holds the pieces of biodata via the particular sequencing of the nucleobases, i.e. adenine (A), cytosine (C), guanine (G), and thymine (T) in DNA or its demethylated analogue uracil (U) in RNA.

Nowadays, our understanding of the structures, topologies, and functions of nucleobase assemblies have been expanded and detailed to a high resolution; thanks to the continuous evolution of the computational sciences, the investigation of the genes' or alleles' functional interactions can be approached [4]. Also, our capability to manipulate the genetic information has been notably improved by the development of the clustered regularly interspaced short palindromic repeats (CRISPR) technologies, for example, by providing novel approaches to the treatment of cancer [5]. Therefore, several evidences have highlighted the clinical relevance of less common RNA topologies, such as circular RNA or noncoding RNA fragments as markers and/or potential targets for the development of new therapies [6,7].

The inhibition of a correct functioning of DNA or RNA molecules is a robust technique in medicinal chemistry since it results into the major effects on the cell homeostasis and causes apoptosis. On the other hand, the drugs, designed for targeting other cellular functions, may still attack the DNA and RNA polymers, thus producing the unintended side effects [8,9].

Most anticancer drugs are formulated expressly for attacking DNA or proteins [10–12], whereas the therapeutic agents aiming at RNA are less

* Corresponding author.
E-mail address: tolbatov.i@gmail.com (I. Tolbatov).

https://doi.org/10.1016/j.jmgm.2024.108806
Received 20 February 2024; Received in revised form 21 May 2024; Accepted 28 May 2024
Available online 31 May 2024

numerous [13,14]. It is quite surprising since the RNA molecules are essential for correct metastasis in cells, both eukaryotic and bacterial, as well as in viruses. Although the DNA and RNA consist of the same nucleobases, their secondary and tertiary structure differs greatly, thus permitting the conception of the drugs selective for only DNA or RNA targets [15]. One of the possible strategies here is the formulation of drugs with the activation profiles designed either for the activation happening in the cytoplasm or in the nucleus [16]. Presumably, in the first case, the drugs will target RNA, whereas in the latter case, they should predominantly target the nucleus, thus, DNA would be a more likely target.

Both the chemical constituents of the nucleoside biopolymers and their secondary and tertiary geometrical configurations allow for the rational design of a drug preventing the cellular dispatch of the correct bit of biodata [17,18]. There exist two possible strategies to this end. Firstly, it is feasible to alter the nucleobase in vivo by coordinating a drug to it, the nucleobase then changes its chemical properties due to the presence of a drug, thus, the whole chain of biopolymer will not be able to properly fulfil its biological role [19]. The other way is the in vitro synthesis of a nucleobase distorted by appending of a drug which is to be administered into the cell afterwards. The modified nucleobase becomes then included in the biopolymers, which become distorted in their turn by the presence of an altered nucleobase [20]. Indeed, there exists a category of the nucleoside therapeutic agents designed for the treatment of cancers, viral and bacterial infections. They mimic the native nucleosides, become included in the DNA and RNA biopolymers yielding them debilitated [21–24].

Metal complexes with medicinal effects, also known as metallodrugs, are among the drugs intended specifically for the attack onto nucleosides [25]. The textbook example of such a metallodrug is the cisplatin, $[Pt(NH_3)_2Cl_2]$, a complex with the discovery of the cytotoxic features of which the modern bioinorganic chemistry started [26]. Its mode of action includes the activation via the replacement of one or two chlorides by the water molecules. The activated complex possesses an enhanced selectivity to purine bases, especially to N_7 of guanine [27,28]. The success of cisplatin and the wont to circumvent its severe toxic side effects have caused a great progress in this subfield, which resulted in the conception of novel metallodrugs based on Pt or other transition metals [29–31]. Ruthenium is among the most ubiquitous metals utilized in the formulation of novel metallodrugs, and it gives great results. For example, the Ru-based drugs NAMI-A and KP1019 have recently attained the elevated stages of clinical tests [32,33].

The diruthenium (II,III) and dirhodium (II,II) paddlewheel complexes consist of the bimetallic core and the bridging carboxylate ligands arranged in a lantern-like fashion (Fig. 1), their general formula being $[M_2(O_2CR)_4]L_2$ (M = Rh, Ru; R=CH_3^-, $CH_3CH_2^-$, etc., L = solvent molecule or anionic ligand). Their high cytotoxicity has been showcased in a myriad of recent studies [34–37]. The diRu and diRh paddlewheel complexes feature a different nature of the intermetallic bond. The diRu core has a mixed valence (II,III) due to the availability of three uncoupled electrons on antibonding metal–metal orbitals, thus, each Ru atom has a charge of +2.5 [38]. On the other hand, the core of diRh complex includes an intermetallic bond of the first order, assigning the valence (II,II) to this complex. These differences produce the crucial distinctness in the selectivity of these paddlewheel complexes.

The Ru-based paddlewheel analogue $[Ru_2(\mu\text{-}O_2CCH_3)_4Cl]$ binds to aspartate side chains of the model protein hen egg white lysozyme [39]. The usage of therapeutic ligands with the acetate motif, such as dipeptides, non-steroidal anti-inflammatory drugs (NSAIDs), or fatty acids, allowed to obtain the complexes with anti-inflammatory and cytotoxic properties [40,41]. Its Rh-based analogue $[Rh_2(\mu\text{-}O_2CCH_3)_4]$ was found to target the side chains of Asn, Asp, His, Lys, and the C-terminal carboxylate in proteins [42–44]. The diRh paddlewheel complex is active against a plethora of cancers, such as sarcoma 180 [45], P388 leukemia [45], L1210 tumors [46], and Ehrlich-Lettre ascites carcinoma [47–49]. However, it is very toxic due to the harsh side-effects.

In the present investigation, we studied the coordination at the DNA and RNA nucleobases of the $[Ru_2(\mu\text{-}O_2CCH_3)_4(H_2O)Cl]$, $[Ru_2(\mu\text{-}O_2CCH_3)_4(OH)Cl]$, and $[Rh_2(\mu\text{-}O_2CCH_3)_4(H_2O)_2]$ complexes (Fig. 1). We studied the reactions yielding the metalation of the nucleobases by these complexes. We always considered the exchange of an axial ligand with the attacked nucleobase. In case of the complex $[Ru_2(\mu\text{-}O_2CCH_3)_4(H_2O)Cl]$, we analyzed both the reactions resulting in the loss of chloride or water (reactions 1 and 2). The diaquo complex in high pH by means of deprotonation of the axial aquo ligand transforms into the complex $[Ru_2(\mu\text{-}O_2CCH_3)_4(OH)Cl]$. We considered only the loss of axial chloride for this complex (reaction 3). The substitution reaction of the complex $[Rh_2(\mu\text{-}O_2CCH_3)_4(H_2O)_2]$ can happen only via the loss of the aquo ligand in the axial position (reaction 4).

We analyzed the structural impact of the metalation by these complexes on the stability of the polynucleotide structure by using the density functional theory (DFT) methodology. We studied the selectivity of the diRu and diRh complexes towards A, C, G, T, and U by assuming possible the coordination at all existing pyridyl nitrogens. We also studied whether this metalation may alter the complementarity of nucleobases. Moreover, we evaluated whether the binding of a diRu or diRh paddlewheel complex to a nucleobase may affect the coordination of the bridging acetates and induce their detachment, a property of these complexes which makes them the promising double-action drug candidates. Our computational study formulated an important rationale for future experimental and theoretical studies onto the interactions of diRu and diRh paddlewheel complexes with DNA and RNA.

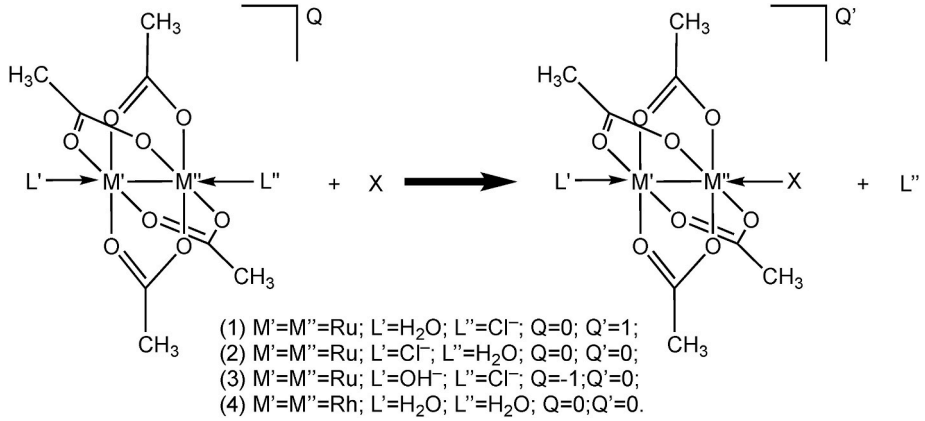

Fig. 1. Studied substitution reactions (1)–(4). Attacked nucleophile is denoted by X and represents nucleobases A, C, G, Ta, Tb, Ua, Ub, and nucleobase pairs AT, AU, GC.

2. Computational details

All the calculations were carried out by the Gaussian 16 quantum chemistry package [50]. DFT permits the accurate analysis of reactions of transition metal complexes [51–53], encompassing Ru and Rh [54–56]. The hybrid range-corrected functional ωB97X-D [57] was used for all optimizations together with the basis set def2SVP basis set [58,59], the employed functional is recognized to produce the trustworthy geometries and accurate evaluation of the electronic and solvation energies [60,61]. The same computational scheme has been previously adopted to investigate the thermodynamics and kinetics of the reaction of diruthenium and dirhodium paddlewheel complexes with protein sites [62,63]. Therefore, we repute adequate the ωB97X-D/def2SVP level of theory being the energy evaluations devoted to rank either the metal-nucleobase interactions or the base complementarities within the base pairs' complexes (vide infra), i.e. by performing relativistic comparisons within sets of congeneric complexes. The stationary nature of the minima was checked by the frequency calculations which also allowed the computation of zero-point energy (ZPE) and vibrational corrections to the thermodynamic properties via the harmonic approximation as well as the Gibbs free energy for each structure. The solvation free energy in water was described by the Polarizable Continuum Model using the integral equation formalism variant (IEFPCM) technique [64], this method producing accurate free energies both for neutral and charged complexes [65]. We used experimental values for the solvation energies −6.3 and −74.5 kcal/mol for water [66] and chloride [67], respectively.

Snapping energies of acetate for the diRu and diRh paddlewheel complexes were calculated for all 4 acetates in each case, only the one with the lowest snapping energy was reported.

The Natural Bond Orbital (NBO) analysis [68], performed in water at the level ωB97X-D/def2SVP, allowed the assessment of the strength of the hydrogen bond interactions in either free or metalated nucleobase pairs.

3. Results and discussion

The binding of either diRu or diRh paddlewheel scaffolds to the nucleophile sites available on the nucleobase moieties of DNA and RNA was modelled by assuming the substitution of one axial ligand as the early chemical event, following the logic of previous investigations [62,63]. The $[Ru_2(\mu\text{-}O_2CCH_3)_4]^+$ and $Rh_2(\mu\text{-}O_2CCH_3)_4$ metal fragments, composed of the bimetallic moiety and four equatorial carboxylate ligands, were coordinated by aquo and/or chloride axial ligands assumed to be labile.

The four substitution reactions of diRu and diRh paddlewheel complexes with the nucleobases were summarized in Fig. 1. The substitution of the chloro or aquo ligand in the $Ru_2(\mu\text{-}O_2CCH_3)_4(H_2O)Cl$ complex were modelled via processes (1) and (2), respectively. The formation of the latter aquo-chloro diRu complex has been hypothesized to parallel the dissolution of $Ru_2(\mu\text{-}O_2CCH_3)_4(H_2O)Cl$ (s) in neutral/acidic aqueous media, whereas at higher pH, the formation of $[Ru_2(\mu\text{-}O_2CCH_3)_4(HO)Cl]^-$ anionic species cannot be excluded. Hence, the reactions of $[Ru_2(\mu\text{-}O_2CCH_3)_4(HO)Cl]^-$ with nucleobase scaffolds were also modelled via the substitution of the chloro ligand, i.e. via the process (3) (Fig. 1).

The diRh tetra-carboxylate complex was assumed in the biaquo form $Rh_2(\mu\text{-}O_2CCH_3)_4(H_2O)_2$ and the substitution of one aquo ligand by nucleobase scaffolds were modelled via the process (4) (Fig. 1).

Both pyrimidine and purine nucleobases are characterized by several nucleophile sites amenable to the metal coordination and potentially able to replace either aquo or chloro axial ligands from diRu or diRh paddlewheel complexes. The amenable metal binding atoms on the nucleobase scaffolds are either decorating or part of the five and/or six-membered rings (Fig. 2). Despite the oxo or amino groups decorating the nucleobases, cyclic structures (red, Fig. 2) may in principle replace the labile aquo ligands in the considered diRu and diRh complexes since the metal coordination ability of these groups is commonly assumed to be negligible because of their participation in the inter-nucleobase hydrogen bond interactions. On the other hand, the pyridyl nitrogen atoms (green, Fig. 2) feature a higher metal coordination ability and, in the case of the adenine and guanine N_7, a high bulk exposure since they are not involved in the hydrogen bond base pairing. For the thymine and uracil nucleobases, being deprived of any pyridyl site, the tautomeric equilibrium is assumed to form the corresponding Tb and Ub species, converting the non-coordinating site NH (blue, Fig. 2) into the metal binding N_1 (green, Fig. 2) at a free energy cost of about 13 kcal/mol.

The thermodynamics of the processes (1)–(4) involving single nucleobase scaffolds was investigated at DFT level of theory, and the calculated reaction Gibbs free energies (GFEs) were reported in Table 1. As shown, our calculations clearly demonstrated a remarkable difference between the highly endergonic chloro substitution for the processes (1) and (3) and the largely exergonic (2) and (4) processes involving the substitution of the axial aquo ligand in diRu and diRh paddlewheel complexes.

The reactions (2) and (4) of thymine and uracil nucleobases, as well as the reaction (2) of the guanine via the metal coordination of the N_3,

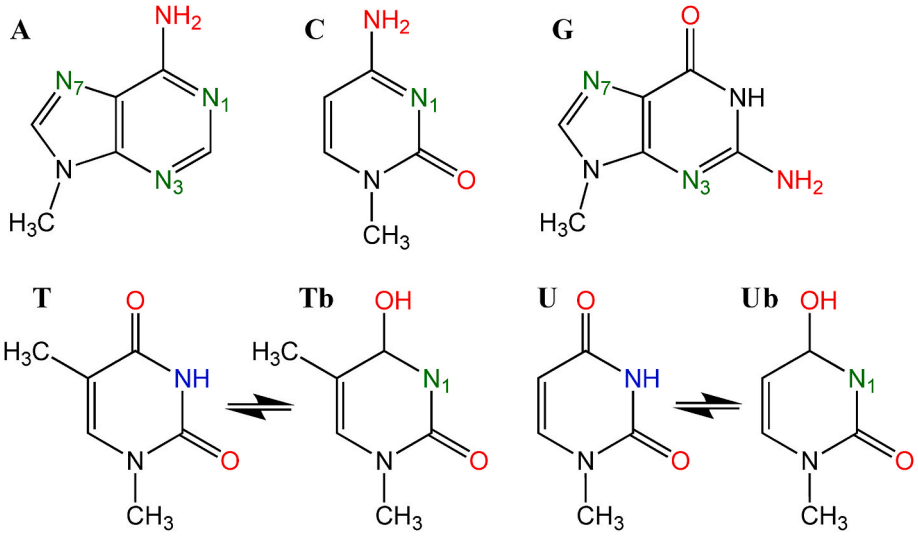

Fig. 2. The nucleobases attacking the axial positions of paddlewheel complexes via the numbered nucleophile pyridyl nitrogen atoms. The two tautomers of T and U, i.e. Tb and Ub, respectively, present the N_1 nucleophile site.

Table 1
GFE values for the substitution reactions (1)–(4) in kcal/mol. The position of the nucleobase at which the metalation occurs is indicated (superscript).

Nucleobase	Substitution reaction			
	(1)	(2)	(3)	(4)
A^1	19.7	−6.8	11.3	−10.9
A^3	24.0	−2.6	12.6	−6.5
A^7	19.2	−8.1	10.1	−10.0
C^1	21.9	−3.4	14.7	−6.3
G^3	26.6	0.0	15.0	−5.6
G^7	19.8	−5.9	14.7	−10.0
Tb^1	35.1	8.5	27.8	3.3
Ub^1	35.6	8.6	25.1	4.7

were found to be endergonic (Table 1), whereas in all other cases, the processes (2) and (4) resulted to be exergonic. As a general trend, we recorded the higher exergodicity of process (4) compared to (2), indicating that the diRh, compared to the diRu scaffold, reacts more favorably with nucleobases.

Also, the purines, adenine and guanine, were found to react more favorably. These data corroborated the well-known role of these nucleobases in the binding of a transition metal complex cisplatin which has been found to bind DNA almost exclusively to the N_7 of these nucleobases [27,69]. Interestingly, the reaction (4) of A^1 resulted more exergonic compared to A^7, whereas the reaction (2) of A^7 resulted to be the most favored. These data may reflect a higher preference for the adenine nucleobase disclosed by both diRu and diRh paddlewheel complexes and for the N_7 and N_1 pyridyl sites of this nucleobase, respectively. More precisely, the reaction of the diRu scaffold with the most amenable adenine site, i.e. A^7, was more exergodic by about 2 kcal/mol (Table 1) compared to G^7; these data would translate in an A^7:G^7 binding ratio of about 29:1. On the other hand, in the reaction of the diRh with adenine and guanine nucleobases, although generally more exergonic, the free energy difference between A^1 and G^7 is only −0.9 kcal/mol (Table 1) that would translate in a lower A^1:G^7 binding ratio of about 4:1. The reactions (2) and (4) of the cytosine nucleobase, although exergonic in both cases, resulted to be always less exergonic by 2–4 kcal/mol compared to the purine nucleobases – purine:pyrimidine binding ratio higher than 100:1 – hence, our calculations eventually corroborated that adenine and guanine are the most favorable nucleobase binding sites to diRu and diRh paddlewheel complexes.

The order of favorability of metalation of various nitrogens in the studied nucleobases can be also seen from the calculation of relative bond Gibbs free energies for the 4 metalated complexes $[Ru_2(\mu\text{-}O_2CCH_3)_4(H_2O)NB]^+$, $Ru_2(\mu\text{-}O_2CCH_3)_4Cl(NB)$, $[Ru_2(\mu\text{-}O_2CCH_3)_4(HO)NB]^+$, and $Rh_2(\mu\text{-}O_2CCH_3)_4(H_2O)(NB)$, formed via the substitution reactions (1)–(4), respectively (Table S1, NB denotes a metalated nucleobase). As expected, the relative bond free energy data paralleled the trends of substitution free energies, thus corroborating the conclusions based on Table 1.

The higher favorability of processes (2) and (4) involving the purine nucleobases paves the way to targeting of biomolecules bearing not only single nucleobases, e.g. nucleotide cofactors such as adenosine triphosphate (ATP), guanosine monophosphate (GMP), nicotinamide adenine dinucleotide (NAD), etc., or unpaired nucleobases in single stranded RNA, but also paired nucleobases in double stranded DNA or RNA. To better elucidate the impact of nucleobase pairing on the reaction with diRu and diRh scaffolds, the thermodynamics of reactions (1)–(4) was investigated when the AT, AU and GC base pairs coordinate at the axial position of diRu and diRh scaffolds.

On overall, calculations showed that the nucleobase pairs reacted less favorably compared to single nucleobases with paddlewheel complexes, as testified by the slight increase of the GFE values (Table 2). Although the lower affinity toward the bimetallic scaffolds was not uniform, G^7 and A^7 were confirmed to be the most favorable metalation sites on the nucleobase pairs. Moreover, the preference for the binding of

Table 2
GFE values for the substitution reactions with the nucleobase pairs.

Nucleobase pair	Substitution reaction			
	(1)	(2)	(3)	(4)
$AT(A^3)$	25.3	−1.8	14.2	−4.4
$AT(A^7)$	21.7	−4.4	11.8	−8.5
$AU(A^3)$	24.6	−1.9	13.7	−4.7
$AU(A^7)$	21.5	−5.9	11.8	−8.8
$GC(G^3)$	26.7	−1.1	14.5	−3.6
$GC(G^7)$	20.9	−4.7	11.1	−4.3

the adenine nucleobase in the AU and AT over the GC pair was also confirmed. Again, the diRh paddlewheel scaffold disclosed a higher preference for the adenine nucleobase, the reaction of either AT or AU pair resulted to be more exergodic by at least 4 kcal/mol compared to the GC pair. Interestingly, calculations evidenced the highest exergodicity for the reaction (2) of the diRu paddlewheel complex with AU (A^7), and GFE value of 1.5 kcal/mol lower than the value for the reaction with the $AT(A^7)$ pair, which correspond to an $AU(A^7)$:$AT(A^7)$ binding ratio of about 12:1 and, more importantly, indicate a rare example of RNA selective metalation.

The response of nucleobase pairs upon coordination at diRu or diRh bimetallic scaffolds was also investigated by the estimate of the base pairing interaction energy. Although quantitative estimates of the base pairing energies were not expected at the employed level of theory, we envision that a qualitative insight of the energy trends and comparisons was correctly gained. On overall, we found that the coordination of both diRu and diRh fragments induces a weakening of the corresponding base pairing interaction (Table 3).

It is worth focusing on the trends of pairing interactions affecting the $AU(A^7)$, $AT(A^7)$ and $GC(G^7)$ systems that were found to most favorably coordinate the diRu and diRh scaffolds (data in bold, Table 3). The AT (A^7) and $AU(A^7)$ pairing interactions are more sensibly weakened by the coordination of the diRu compared to the diRh scaffold, i.e. the base pairing interaction decreases by −58 %, whereas the decrease in the GC (G^7) complex is only −11 %. On the other hand, the coordination of the diRh scaffold determined a more pronounced weakening of the $GC(G^7)$ base pairing, i.e. −59 %, while the $AU(A^7)$ and $AT(A^7)$ pairs were affected by only −30 and −33 % (Table 3). The different response of the base pairing interaction to the binding of diRu and diRh paddlewheel scaffolds may be ascribed to a different modulation of the hydrogen bonds patterns involving the metalated nucleobase. Indeed, the AT and AU base pairs are held by two hydrogen bond interactions in which the adenine base plays the donor and the acceptor role by means of the 6-amino and N_3 groups, respectively (Fig. 3). On the other hand, the guanine base in the GC pair forms three hydrogen bond interactions, two donor and one acceptor interactions, involving the 2-amino and NH groups (donor) and the 6-oxo group (acceptor) (Fig. 3). We envision that the binding of metal fragments on the N_7 may cause the fading of both the hydrogen bond acceptor and donor attitudes in the nucleobase because of the electron withdrawing effect commonly ascribed to metallic fragments. Instead, the different responses of the adenine versus

Table 3
GFE values for uncoupling non-metalated and metalated nucleobase pairs (in kcal/mol). The percentage loss of pairing interaction upon diRu or diRh coordination is also reported (in parentheses).

Nucleobase pair	Metalation process		No metal
	(2)	(4)	
$AT(A^3)$	3.0 (−30 %)	2.3 (−47 %)	4.3
$AT(A^7)$	1.8 (−58 %)	2.9 (−33 %)	
$AU(A^3)$	3.4 (−15 %)	2.2 (−45 %)	4.0
$AU(A^7)$	1.7 (−58 %)	2.8 (−30 %)	
$GC(G^3)$	9.5 (−2%)	7.6 (−23 %)	9.7
$GC(G^7)$	8.6 (−11 %)	4.0 (−59 %)	

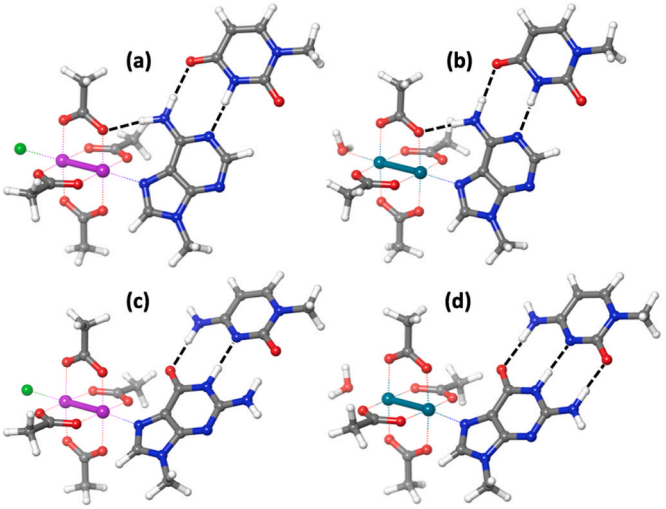

Fig. 3. Ball-and-sticks representation of the diRu complexes coordinated with AU(A^7) **(a)** and GC(G^7) nucleobase pairs **(c)** and diRh complexes of AU(A^7) **(b)** and GC(G^7) **(d)**. Hydrogen bond interactions are depicted as black dashed lines. Color scheme: Rh (dark green), Ru (plum), Cl (light green), O (red), N (blue), C (grey), H (white). (For interpretation of the references to colour in this figure legend, the reader is referred to the Web version of this article.)

guanine base pairs to metalation could rather be determined by the presence of non-covalent interactions between the paddlewheel moieties and the bound nucleobase. Indeed, the close spatial proximity of the 6-amino group of adenine and the μ-bridged carboxylate ligands may eventuate in the formation of a hydrogen bond. Beside evidently stabilizing the metal-nucleobase coordination, such a hydrogen bond is expected to also tune the hydrogen bond acceptor attitude of the adenine 6-amino group. Therefore, the formation of such a strong non-covalent interaction in either AU(A^7) or AT(A^7) complexes may modulate the reciprocal orientation of the paddlewheel scaffold toward the bound nucleobase.

To better analyze these aspects, the optimized geometries of the diRu and diRh complexes (via processes (2) and (4), respectively) with either single or paired adenine and guanine scaffolds were inspected, and the relevant geometrical parameters were summarized in Table 4. As expected, the hydrogen bond interaction between the 6-amino group and one μ-bridged carboxylate was retrieved in all diRh and diRu complexes of the adenine nucleobase, whereas no hydrogen bond was detected in the guanine complexes. The N–H···O(carboxylate) distances in the adenine complexes were found to be well below 2 Å, even though slightly lower values, testifying stronger interactions, were detected in the diRh complexes (Table 4). Therefore, the coordinating nucleobase was found to approach the diRu and diRh scaffolds with slightly different angular orientations: the coordinating adenine resulted more eclipsed than guanine, as shown by the lower O(OAc)-*M*-N_7-C_6 dihedral angles. Therefore, adenine is even more eclipsed upon coordination at the diRh scaffold probably because of a more effective orbital overlapping between the two approaching moieties. These results are totally in line with above discussed GFE values for the processes (2) and (4), indicating stronger diRh-adenine interactions compared to diRu-adenine. To further corroborate this view, natural bonding orbital (NBO) analyses were carried out on the diRu and diRh complexes of the adenine nucleobase (Table 4). In particular, the second order perturbation NBO analysis of both diRh and diRu complexes showed a stronger orbital interaction between an occupied orbital (labelled LP in the NBO scheme) located on the carboxylate oxygen and an unoccupied orbital (labelled BD* in the NBO scheme) ascribed to the antibonding combination between an sp^2 orbital of the N and an s orbital on the H atom of the 6-amino group (Table 4). Importantly, such an analysis showed this orbital interaction to be in the 14.2–15.7 kcal/mol range for the diRh complexes, whereas it falls in the 9.0–10.5 kcal/mol range when the diRu complexes are concerned. Thus, the hydrogen bond between the paddlewheel scaffold and the coordinated adenine is at least 50 % stronger in the diRh compared to diRu complexes.

Table 4
Structural parameters for the metalated A, AT, AU, and GC (products of substitution reactions 2 and 4) and energies of the hydrogen bonds. Distances in Å, dihedral angle in degrees, energy of the H-bonds in kcal/mol. Always the closest acetate is considered. N indicates the atom to which the metal complex is attached (N_1 or N_7).

Complex	Structural parameters		Energy of H-bond
	Distance O(OAc)-H(NH_2)	dihedral O(OAc)-*M*-N-C_6	O(OAc)-H (NH_2)
[Ru_2(μ-O_2CCH_3)$_4$Cl (A^1)]	1.91	29.33	9.00
[Rh_2(μ-O_2CCH_3)$_4$(H_2O) (A^1)]	1.82	16.70	14.20
[Ru_2(μ-O_2CCH_3)$_4$Cl (A^7)]	1.88	31.00	10.51
[Rh_2(μ-O_2CCH_3)$_4$(H_2O) (A^7)]	1.81	22.88	14.93
[Ru_2(μ-O_2CCH_3)$_4$Cl (A^7T)]	1.88	33.34	9.89
[Rh_2(μ-O_2CCH_3)$_4$(H_2O) (A^7T)]	1.81	20.02	15.68
[Ru_2(μ-O_2CCH_3)$_4$Cl (A^7U)]	1.89	34.20	9.84
[Rh_2(μ-O_2CCH_3)$_4$(H_2O) (A^7U)]	1.81	22.02	15.22
[Ru_2(μ-O_2CCH_3)$_4$Cl (G^7C)]	n/a	44.28	n/a
[Rh_2(μ-O_2CCH_3)$_4$(H_2O) (G^7C)]	n/a	45.49	n/a

In order to estimate the effect of binding of a diRu or diRh paddlewheel complex to a nucleobase onto the facileness with which a bridging acetate may detach, we calculated the GFE energies for the cleavage of one acetate, without taking into account the relaxation of the structures, which follows the acetate detachment. Since there are four bridging acetates in each structure, each with a different detachment energy, only the lowest energy values are presented in Table 5. The coordination of a nucleobase at the axial position decreased the energy by 11.1–18.8 kcal/mol for the acetate detachment in the structures [Ru_2(μ-O_2CCH_3)$_4$(H_2O)(NB)] and [Ru_2(μ-O_2CCH_3)$_4$Cl(NB)] produced in the reactions (1) and (2), respectively. The greatest diminishing of energy occurred for the products of reaction (2), indeed, the coordination of nucleobases decreased the energy by 15.8–18.8 kcal/mol. On the other hand, the reaction (3) increased the detachment energy by 3.3 kcal/mol, whereas

Table 5
GFE energy values for the dissociation of one acetate for the diRu and diRh paddlewheel complexes (last row) and paddlewheel complexes attached to nucleobases. Energies are calculated for the non-relaxed complexes. Values in kcal/mol.

Nucleobase (NB)	Structure, reaction			
	Ru_2(μ-O_2CCH_3)$_4$(H_2O)(NB)]$^+$, (1)	[Ru_2(μ-O_2CCH_3)$_4$Cl(NB)], (2)	Ru_2(μ-O_2CCH_3)$_4$(OH)(NB)], (3)	[Rh_2(μ-O_2CCH_3)$_4$(H_2O)(NB)], (4)
A^7	101.0	95.5	89.9	85.1
C^1	98.8	93.4	88.9	83.7
G^7	98.0	93.6	89.4	83.8
Tb^1	101.1	96.4	90.7	85.6
Ub^1	100.2	95.1	91.1	85.0
Ref. values for non-attached paddlewheel	112.2	112.2	85.6	85.2

the reaction (4) did not appreciably affect the bond the acetate coordination strength. We can conclude that the coordination of a diRh complex to a nucleobase does not ease the subsequent cleavage of acetate, while the coordination of diRu complex in a substitution reaction (2), resulting in the presence of chloride and nucleobase in the axial positions of the complex, substantially facilitates the detachment of acetate. The occurrence of this effect corroborates the concept of the diRu paddlewheel complex as a promising dual acting drug candidate or a drug with the targeted delivery. Indeed, the initial coordination at a nucleobase weakens the diRu-acetate bonds, favoring the release of the acetate. If the acetate is substituted by an active pharmacophore, then its release will be targeted and will happen only after the attachment to a nucleobase.

4. Conclusions

To resume, the structural insight provided by our calculations evidenced how diRu and diRh paddlewheel complexes can bind preferentially to the adenine nucleobase, either in the single or paired form, through the formation of a hydrogen bond between the 6-amino group of the nucleobase and one equatorial carboxylate ligand, in full agreement with the available experimental data [70]. Moreover, we showed how the diRh compared to diRu is able to coordinate at the pyridyl nitrogen sites of nucleobases more tightly, thus resulting to be probably more cytotoxic. On the other hand, the diRu scaffold was found to be bound less and, curiously, more selectively to nucleobase targets. Interestingly, we appreciated how diRu may coordinate more tightly the AU compared to the AT nucleobase pair, thus being a rare example of RNA-selectivity. Based on our study, we can tentatively depict the diRh compared to the diRu scaffold as more potent and less selective in the binding of nucleobases, being the N_7 of adenine the preferential coordinative site.

CRediT authorship contribution statement

Iogann Tolbatov: Writing – original draft, Investigation, Formal analysis, Conceptualization. **Paolo Umari:** Writing – review & editing. **Alessandro Marrone:** Writing – review & editing, Investigation, Formal analysis, Conceptualization.

Declaration of competing interest

The authors declare that they have no known competing financial interests or personal relationships that could have appeared to influence the work reported in this paper.

Data availability

Data will be made available on request.

Acknowledgements

This work has been funded by the European Union - Next-Generation EU ("PNRR M4C2-Investimento 1.4- CN00000041"). We acknowledge the CINECA award under the ISCRA initiative, for the availability of high performance computing resources and support. IT gratefully acknowledges the usage of HPC resources from Direction du Numérique – Centre de Calcul de l'Université de Bourgogne (DNUM CCUB).

Appendix A. Supplementary data

Supplementary data to this article can be found online at https://doi.org/10.1016/j.jmgm.2024.108806.

References

[1] Y. Hu, B. Stillman, Origins of DNA replication in eukaryotes, Mol. Cell 83 (3) (2023) 352–372, https://doi.org/10.1016/j.molcel.2022.12.024.
[2] G. Faure, A.Y. Ogurtsov, S.A. Shabalina, E.V. Koonin, Role of mRNA structure in the control of protein folding, Nucleic Acids Res. 44 (22) (2016) 10898–10911, https://doi.org/10.1093/nar/gkw671.
[3] A.F. Palazzo, E.S. Lee, Non-coding RNA: what is functional and what is junk? Front. Genet. 6 (2015) 2, https://doi.org/10.3389/fgene.2015.00002.
[4] J. Li, J. Luo, L. Liu, H. Fu, L. Tang, The genetic association between apolipoprotein E gene polymorphism and Parkinson disease: a meta-Analysis of 47 studies, Medicine 97 (43) (2018) e12884, https://doi.org/10.1097/MD.0000000000012884.
[5] D. Wang, X.W. Wang, X.C. Peng, Y. Xiang, S.B. Song, Y.Y. Wang, L. Chen, V.W. Xin, Y.N. Lyu, J. Ji, Z.W. Ma, CRISPR/Cas9 genome editing technology significantly accelerated herpes simplex virus research, Cancer Gene Ther. 25 (5) (2018) 93–105, https://doi.org/10.1038/s41417-018-0016-3.
[6] X.L. Xue, S. Zhao, M.C. Xu, Y. Li, W.F. Liu, H.Z. Qin, Circular RNA_0000326 accelerates breast cancer development via modulation of the miR-9-3p/YAP1 axis, Neoplasma 70 (3) (2023) 430–442, https://doi.org/10.4149/neo_2023_220904N894.
[7] L. Tang, Y. Wang, J. Xiang, D. Yang, Y. Zhang, Q. Xiang, J. Li, lncRNA and circRNA expression profiles in the hippocampus of Aβ 25-35-induced AD mice treated with Tripterygium glycoside, Exp. Ther. Med. 26 (3) (2023) 426, https://doi.org/10.3892/etm.2023.12125.
[8] G. Bischoff, S. Hoffmann, DNA-binding of drugs used in medicinal therapies, Curr. Med. Chem. 9 (3) (2002) 321–348, https://doi.org/10.2174/0929867023371085.
[9] J.M. Sasso, B.J. Ambrose, R. Tenchov, R.S. Datta, M.T. Basel, R.K. DeLong, Q. A. Zhou, The progress and promise of RNA medicine — an arsenal of targeted treatments, J. Med. Chem. 65 (10) (2022) 6975–7015, https://doi.org/10.1021/acs.jmedchem.2c00024.
[10] V. Brabec, O. Hrabina, J. Kasparkova, Cytotoxic platinum coordination compounds. DNA binding agents, Coord. Chem. Rev. 351 (2017) 2–31, https://doi.org/10.1016/j.ccr.2017.04.013.
[11] B.A. Carneiro, W.S. El-Deiry, Targeting apoptosis in cancer therapy, Nat. Rev. Clin. Oncol. 17 (7) (2020) 395–417, https://doi.org/10.1038/s41571-020-0341-y.
[12] A.R. Timerbaev, C.G. Hartinger, S.S. Aleksenko, B.K. Keppler, Interactions of antitumor metallodrugs with serum proteins: advances in characterization using modern analytical methodology, Chem. Rev. 106 (6) (2006) 2224–2248, https://doi.org/10.1021/cr040704h.
[13] L. Chen, G.A. Calin, S. Zhang, Novel insights of structure-based modeling for RNA-targeted drug discovery, J. Chem. Inf. Model. 52 (10) (2012) 2741–2753, https://doi.org/10.1021/ci300320t.
[14] A.E. Hargrove, Small molecule–RNA targeting: starting with the fundamentals, Chem. Commun. 56 (94) (2020) 14744–14756, https://doi.org/10.1039/D0CC06796B.
[15] D.J. Huggins, W. Sherman, B. Tidor, Rational approaches to improving selectivity in drug design, J. Med. Chem. 55 (4) (2012) 1424–1444, https://doi.org/10.1021/jm2010332.
[16] K.D. Warner, C.E. Hajdin, K.M. Weeks, Principles for targeting RNA with drug-like small molecules, Nat. Rev. Drug Discov. 17 (8) (2018) 547–558, https://doi.org/10.1038/nrd.2018.93.
[17] M.J. O'Connor, Targeting the DNA damage response in cancer, Mol. Cell 60 (4) (2015) 547–560, https://doi.org/10.1016/j.molcel.2015.10.040.
[18] S.T. Crooke, J.L. Witztum, C.F. Bennett, B.F. Baker, RNA-targeted therapeutics, Cell Metabol. 27 (4) (2018) 714–739, https://doi.org/10.1016/j.cmet.2018.03.004.
[19] A.M. Yu, Y.H. Choi, M.J. Tu, RNA drugs and RNA targets for small molecules: principles, progress, and challenges, Pharmacol. Rev. 72 (4) (2020) 862–898, https://doi.org/10.1124/pr.120.019554.
[20] K. Paunovska, D. Loughrey, J.E. Dahlman, Drug delivery systems for RNA therapeutics, Nat. Rev. Genet. 23 (5) (2022) 265–280, https://doi.org/10.1038/s41576-021-00439-4.
[21] R. Taylor, P. Kotian, T. Warren, R. Panchal, S. Bavari, J. Julander, S. Dobo, A. Rose, Y. El-Kattan, B. Taubenheim, Y. Babu, BCX4430–a broad-spectrum antiviral adenosine nucleoside analog under development for the treatment of Ebola virus disease, J. Infect. Publ. Health 9 (3) (2016) 220–226, https://doi.org/10.1016/j.jiph.2016.04.002.
[22] R.J. Geraghty, M.T. Aliota, L.F. Bonnac, Broad-spectrum antiviral strategies and nucleoside analogues, Viruses 13 (4) (2021) 667, https://doi.org/10.3390/v13040667.
[23] J.M. Thomson, I.L. Lamont, Nucleoside analogues as antibacterial agents, Front. Microbiol. 10 (2019) 952, https://doi.org/10.3389/fmicb.2019.00952.
[24] M. Guinan, C. Benckendorff, M. Smith, G.J. Miller, Recent advances in the chemical synthesis and evaluation of anticancer nucleoside analogues, Molecules 25 (9) (2020) 2050, https://doi.org/10.3390/molecules25092050.
[25] E.J. Anthony, E.M. Bolitho, H.E. Bridgewater, O.W. Carter, J.M. Donnelly, C. Imberti, E.C. Lant, F. Lermyte, R.J. Needham, M. Palau, P.J. Sadler, Metallodrugs are unique: opportunities and challenges of discovery and development, Chem. Sci. 11 (48) (2020) 12888–12917, https://doi.org/10.1039/D0SC04082G.
[26] P.B. Tchounwou, S. Dasari, F.K. Noubissi, P. Ray, S. Kumar, Advances in our understanding of the molecular mechanisms of action of cisplatin in cancer therapy, J. Exp. Pharmacol. 13 (2021) 303–328, https://doi.org/10.2147/JEP.S267383.
[27] B. Chiavarino, M.E. Crestoni, S. Fornarini, D. Scuderi, J.Y. Salpin, Interaction of cisplatin with adenine and guanine: a combined IRMPD, MS/MS, and theoretical

study, J. Am. Chem. Soc. 135 (4) (2013) 1445–1455, https://doi.org/10.1021/ja309857d.
[28] L.A.S. Costa, T.W. Hambley, W.R. Rocha, W.B. De Almeida, H.F. Dos Santos, Kinetics and structural aspects of the cisplatin interactions with guanine: a quantum mechanical description, Int. J. Quant. Chem. 106 (9) (2006) 2129–2144, https://doi.org/10.1002/qua.20979.
[29] L. Chiaverini, A. Pratesi, D. Cirri, A. Nardinocchi, I. Tolbatov, A. Marrone, M. Di Luca, T. Marzo, D. La Mendola, Anti-staphylococcal activity of the auranofin analogue bearing acetylcysteine in place of the thiosugar: an experimental and theoretical investigation, Molecules 27 (8) (2022) 2578, https://doi.org/10.3390/molecules27082578.
[30] A. Garcia, R.C. Machado, R.M. Grazul, M.T.P. Lopes, C.C. Corrêa, H.F. Dos Santos, M.V. de Almeida, H. Silva, Novel antitumor adamantane–azole gold (I) complexes as potential inhibitors of thioredoxin reductase, J. Biol. Inorg. Chem. 21 (2016) 275–292, https://doi.org/10.1007/s00775-016-1338-y.
[31] S. La Manna, C. Di Natale, V. Panzetta, M. Leone, F.A. Mercurio, I. Cipollone, M. Monti, P.A. Netti, G. Ferraro, A. Terán, A.E. Sánchez-Peláez, S. Herrero, A. Merlino, D. Marasco, A diruthenium metallodrug as a potent inhibitor of amyloid-β aggregation: synergism of mechanisms of action, Inorg. Chem. 63 (1) (2024) 564–575, https://doi.org/10.1021/acs.inorgchem.3c03441.
[32] D. Cirri, T. Marzo, I. Tolbatov, A. Marrone, F. Saladini, I. Vicenti, F. Dragoni, A. Boccuto, L. Messori, In vitro anti-SARS-CoV-2 activity of selected metal compounds and potential molecular basis for their actions based on computational study, Biomolecules 11 (12) (2021) 1858, https://doi.org/10.3390/biom11121858.
[33] E. Alessio, L. Messori, NAMI-A and KP1019/1339, two iconic ruthenium anticancer drug candidates face-to-face: a case story in medicinal inorganic chemistry, Molecules 24 (10) (2019) 1995, https://doi.org/10.3390/molecules24101995.
[34] A. Terán, G. Ferraro, P. Imbimbo, A.E. Sánchez-Peláez, D.M. Monti, S. Herrero, A. Merlino, Steric hindrance and charge influence on the cytotoxic activity and protein binding properties of diruthenium complexes, Int. J. Biol. Macromol. 253 (2023) 126666, https://doi.org/10.1016/j.ijbiomac.2023.126666.
[35] A.M. Angeles-Boza, H.T. Chifotides, J.D. Aguirre, A. Chouai, P.K.L. Fu, K. R. Dunbar, C. Turro, Dirhodium (II, II) complexes: molecular characteristics that affect in vitro activity, J. Med. Chem. 49 (23) (2006) 6841–6847, https://doi.org/10.1021/jm060592h.
[36] R. Hrdina, Dirhodium (II, II) paddlewheel complexes, Eur. J. Inorg. Chem. 2021 (6) (2021) 501–528, https://doi.org/10.1002/ejic.202000955.
[37] T.E. Freitas, R.N. Gomes, A. Colquhoun, D. de Oliveira Silva, Axially-modified paddlewheel diruthenium (II, III)-ibuprofenato metallodrugs and the influence of the structural modification on U87MG and A172 human glioma cell proliferation, apoptosis, mitosis and migration, J. Inorg. Biochem. 165 (2016) 181–191, https://doi.org/10.1016/j.jinorgbio.2016.10.003.
[38] M.A. Aquino, Recent developments in the synthesis and properties of diruthenium tetracarboxylates, Coord. Chem. Rev. 248 (11–12) (2004) 1025–1045, https://doi.org/10.1016/j.ccr.2004.06.016.
[39] L. Messori, T. Marzo, R.N.F. Sanches, D. de Oliveira Silva, A. Merlino, Unusual structural features in the lysozyme derivative of the tetrakis (acetato) chloridodiruthenium (II, III) complex, Angew. Chem. Int. Ed. 53 (24) (2014) 6172–6175, https://doi.org/10.1002/anie.201403337.
[40] I. Tolbatov, E. Barresi, S. Taliani, D. La Mendola, T. Marzo, A. Marrone, Diruthenium (ii, iii) paddlewheel complexes: effects of bridging and axial ligands on anticancer properties, Inorg. Chem. Front. 10 (8) (2023) 2226–2238, https://doi.org/10.1039/D3QI00157A.
[41] D. de Oliveira Silva, Perspectives for novel mixed diruthenium-organic drugs as metallopharmaceuticals in cancer therapy, Anti Cancer Agents Med. Chem. 10 (4) (2010) 312–323, https://doi.org/10.2174/187152010791162333.
[42] G. Ferraro, A. Pratesi, L. Messori, A. Merlino, Protein interactions of dirhodium tetraacetate: a structural study, Dalton Trans. 49 (8) (2020) 2412–2416, https://doi.org/10.1039/C9DT04819G.
[43] D. Loreto, G. Ferraro, A. Merlino, Unusual structural features in the adduct of dirhodium tetraacetate with lysozyme, Int. J. Mol. Sci. 22 (3) (2021) 1496, https://doi.org/10.3390/ijms22031496.
[44] G. Ribeiro, M. Benadiba, A. Colquhoun, D. de Oliveira Silva, Diruthenium (II, III) complexes of ibuprofen, aspirin, naproxen and indomethacin non-steroidal anti-inflammatory drugs: synthesis, characterization and their effects on tumor-cell proliferation, Polyhedron 27 (3) (2008) 1131–1137, https://doi.org/10.1016/j.poly.2007.12.011.
[45] G. Serio, A.P. Kimball, Interaction of rhodium (II) carboxylates with molecules of biologic importance, in: J.L. Bear, H.B. Gray, L. Rainen, I.M. Chang, R. Howard (Eds.), Cancer Chemother. Rep. 59 (3) (1975) 611–620.
[46] R.A. Howard, A.P. Kimball, J.L. Bear, Mechanism of action of tetra-μ-carboxylatodirhodium (II) in L1210 tumor suspension culture, Cancer Res. 39 (7_Part_1) (1979) 2568–2573.
[47] M.S. Nothenberg, S.B. Zyngier, A.M. Giesbrecht, M.T.P. Gambardella, R.H. A. Santos, E. Kimura, R. Najjar, Biological activity and crystallographic study of a rhodium propionate-metronidazole adduct, J. Braz. Chem. Soc. 5 (1) (1994) 23–29.
[48] S. Zyngier, E. Kimura, R. Najjar, Antitumor effects of rhodium (II) citrate in mice bearing Ehrlich tumors, Braz. J. Med. Biol. Res. 22 (3) (1989) 397–401.
[49] A. Erck, L. Rainen, J. Whileyman, I.M. Chang, A.P. Kimball, J. Bear, Studies of rhodium (II) carboxylates as potential antitumor agents, Proc. Soc. Exp. Biol. Med. 145 (4) (1974) 1278–1283, https://doi.org/10.3181/00379727-145-37996.
[50] M.J. Frisch, G.W. Trucks, H.B. Schlegel, et al., Gaussian 16, Revision C.01, Gaussian, Inc., Wallingford CT, 2016.
[51] S. Todisco, M. Latronico, V. Gallo, N. Re, A. Marrone, I. Tolbatov, P. Mastrorilli, Double addition of phenylacetylene onto the mixed bridge phosphinito–phosphanido Pt (i) complex [(PHCy $_2$)Pt(μ-PCy$_2$){κ^{2}P,O-μ-P(O)Cy$_2$}Pt(PHCy$_2$)](Pt–Pt), Dalton Trans. 49 (20) (2020) 6776–6789, https://doi.org/10.1039/D0DT00923G.
[52] R. Paciotti, I. Tolbatov, V. Graziani, A. Marrone, N. Re, C. Coletti, Insights on the activity of platinum-based anticancer complexes through computational methods, in: AIP Conf. Proc., vol. 2040, AIP Publishing, 2018, https://doi.org/10.1063/1.5079061, 1.
[53] I. Tolbatov, A. Marrone, C. Coletti, N. Re, Computational studies of Au (I) and Au (III) anticancer metallodrugs: a survey, Molecules 26 (24) (2021) 7600, https://doi.org/10.3390/molecules26247600.
[54] P. Piazzetta, T. Marino, N. Russo, D.R. Salahub, Direct hydrogenation of carbon dioxide by an artificial reductase obtained by substituting rhodium for zinc in the carbonic anhydrase catalytic center. A mechanistic study, ACS Catal. 5 (9) (2015) 5397–5409, https://doi.org/10.1021/acscatal.5b00185.
[55] I. Tolbatov, A. Marrone, Reactivity of N-heterocyclic carbene half-sandwich Ru-, Os-, Rh-, and Ir-based complexes with cysteine and selenocysteine: a computational study, Inorg. Chem. 61 (1) (2021) 746–754, https://doi.org/10.1021/acs.inorgchem.1c03608.
[56] P. Piazzetta, T. Marino, N. Russo, D.R. Salahub, Explicit water molecules play a key role in the mechanism of rhodium-substituted human carbonic anhydrase, ChemCatChem 9 (6) (2017) 1047–1053, https://doi.org/10.1002/cctc.201601433.
[57] J.-D. Chai, M. Head-Gordon, Long-range corrected hybrid density functionals with damped atom-atom dispersion corrections, Phys. Chem. Chem. Phys. 10 (2008) 6615–6620, https://doi.org/10.1039/B810189B.
[58] D. Andrae, U. Häußermann, M. Dolg, H. Stoll, H. Preuß, Energy-adjusted ab initio pseudopotentials for the second and third row transition elements, Theor. Chim. Acta 77 (1990) 123–141, https://doi.org/10.1007/BF01114537.
[59] F. Weigend, R. Ahlrichs, Balanced basis sets of split valence, triple zeta valence and quadruple zeta valence quality for H to Rn: design and assessment of accuracy, Phys. Chem. Chem. Phys. 7 (18) (2005) 3297–3305, https://doi.org/10.1039/B508541A.
[60] K. Remya, C.H. Suresh, Which density functional is close to CCSD accuracy to describe geometry and interaction energy of small noncovalent dimers? A benchmark study using Gaussian09, J. Comput. Chem. 34 (15) (2013) 1341–1353, https://doi.org/10.1002/jcc.23263.
[61] I. Tolbatov, L. Storchi, A. Marrone, Structural reshaping of the zinc-finger domain of the SARS-CoV-2 nsp13 protein using bismuth (III) ions: a multilevel computational study, Inorg. Chem. 61 (39) (2022) 15664–15677, https://doi.org/10.1021/acs.inorgchem.2c02685.
[62] I. Tolbatov, A. Marrone, Reaction of dirhodium and diruthenium paddlewheel tetraacetate complexes with nucleophilic protein sites: a computational study, Inorg. Chim. Acta. 530 (2022) 120684, https://doi.org/10.1016/j.ica.2021.120684.
[63] I. Tolbatov, A. Marrone, Kinetics of reactions of dirhodium and diruthenium paddlewheel tetraacetate complexes with nucleophilic protein sites: computational insights, Inorg. Chem. 61 (41) (2022) 16421–16429, https://doi.org/10.1021/acs.inorgchem.2c02516.
[64] J. Tomasi, B. Mennucci, E. Cancès, The IEF version of the PCM solvation method: an overview of a new method addressed to study molecular solutes at the QM ab initio level, J. Mol. Struct. THEOCHEM 464 (1–3) (1999) 211–226, https://doi.org/10.1016/S0166-1280(98)00553-3.
[65] A. Klamt, C. Moya, J. Palomar, A comprehensive comparison of the IEFPCM and SS (V) PE continuum solvation methods with the COSMO approach, J. Chem. Theor. Comput. 11 (9) (2015) 4220–4225, https://doi.org/10.1021/acs.jctc.5b00601.
[66] W.L. Jorgensen, J.F. Blake, J.K. Buckner, Free energy of TIP4P water and the free energies of hydration of CH4 and Cl-from statistical perturbation theory, Chem. Phys. 129 (2) (1989) 193–200, https://doi.org/10.1016/0301-0104(89)80004-7.
[67] C.P. Kelly, C.J. Cramer, D.G. Truhlar, Single-ion solvation free energies and the normal hydrogen electrode potential in methanol, acetonitrile, and dimethyl sulfoxide, J. Phys. Chem. B 111 (2) (2007) 408–422, https://doi.org/10.1021/jp065403l.
[68] E.D. Glendening, C.R. Landis, F. Weinhold, NBO 6.0: natural bond orbital analysis program, J. Comput. Chem. 34 (16) (2013) 1429–1437, https://doi.org/10.1002/jcc.23266.
[69] M.H. Baik, R.A. Friesner, S.J. Lippard, Theoretical study of cisplatin binding to purine bases: why does cisplatin prefer guanine over adenine? J. Am. Chem. Soc. 125 (46) (2003) 14082–14092, https://doi.org/10.1021/ja036960d.
[70] H.T. Chifotides, K.R. Dunbar, Interactions of metal−metal-bonded antitumor active complexes with DNA fragments and DNA, Acc. Chem. Res. 38 (2) (2005) 146–156, https://doi.org/10.1021/ar0302078.